arXiv:1208.1850v1 [hep-ph] 9 Aug 2012

Surpassing the 2012 XENON100 exclusion limit with 2011 data and information theory

Jonathan H. Davis,[1] Torsten Enßlin,[2] and Céline Bœhm[1,3]

[1]*Institute for Particle Physics Phenomenology, University of Durham, Durham, DH1 3LE, UK*
[2]*Max-Planck-Institut fur Astrophysik Karl-Schwarzschild-Str. 1. Postfach 13 17 85741 Garching, DE*
[3]*LAPTH, U. de Savoie, CNRS, BP 110, 74941 Annecy-Le-Vieux, France.*

Tremendous progress in the field of dark matter direct detection has allowed modern experiments to reach the sensitivity that is required to exclude large regions of parameter space. The strongest exclusion limit has been set by the XENON100 collaboration which has recently updated the constraint on the dark matter parameter space to an even greater degree. The method used by the collaboration to set this limit is based on a profile Likelihood analysis, which separates the experimental data into bands to better discriminate a potential dark matter nuclear-recoil signal from the electronic-recoil background. However the use of bands is not strictly necessary and tends to make the limit over-conservative. Here we propose an alternative method based on information theory and apply it to the 2011 data-set from the XENON100 experiment. We derive a new exclusion limit with this data which is both stronger than that derived by XENON100 with their profile Likelihood analysis using the same data, and competitive with the new limit which was derived using the recent 2012 data-set.

INTRODUCTION

Despite strong gravitational evidence for the existence of dark matter (DM) in the Universe (from galactic to cluster scales) its nature remains largely a mystery. Yet great progress has been made in this endeavour: direct detection experiments, based on the detection of dark matter induced nuclear recoils have set progressively stronger limits on the properties of dark matter [1, 2], particularly for masses in the GeV to TeV range.

The current world-record limit on the spin-independent cross section for dark matter elastic scattering with nuclei has been set by the XENON100 experiment [3–5], which operates using both liquid and gaseous xenon with a fiducial volume of $\sim 40\,\mathrm{kg}$. The XENON100 detector identifies events by two separate signals [6]: primary (S1) and secondary (S2) scintillation, the former of which is due to scintillation light originating from the liquid part of the detector, while the latter comes from ionised electrons, which drift to the gaseous part of the detector under an electric field. The precision of the detector in identifying and excluding dark matter interactions crucially relies on its ability to discriminate the electronic-recoil (ER) background from nuclear-recoil events (NR), such as those potentially induced by Weakly Interacting Massive Particles (WIMPs), based on their different distributions in S1 and S2.

In order to derive limits on the spin-independent cross section as a function of dark matter mass, the XENON100 collaboration employs a profile Likelihood approach [7, 8]. Such a method takes advantage of the distinct signatures in S1-S2 of electronic and nuclear recoils by splitting the data-space into a number of bands (23 in [8] and 12 in [7]), which allows stronger limits to be placed on the WIMP-nucleon cross section than would otherwise be possible.

Here we point out that in addition to problems associated with systematic uncertainties [9, 10], dividing the S1-S2 space into bands could potentially limit the sensitivity of the analysis, as discrimination is not possible between events within the same band. Hence despite the great achievements of the XENON100 collaboration in setting limits on the WIMP-nucleon cross section, one can try to improve the analytical method, to exploit the full sensitivity of the experiment.

In this letter we propose a Bayesian approach, based on examining the information Hamiltonian. We will demonstrate using the XENON100 data-set from 100 live days of running [4] that not only is this method consistent with the previous results obtained by the use of a profile Likelihood analysis [3, 4, 8] and by a Bayesian analysis performed in [11], but it also leads to an exclusion limit which is stronger with respect to [4, 8, 11] and competitive with [3] where new data is used, due to the use of the full data-space. The analysis using the method presented here of the newest XENON100 data [3] is left to the collaboration themselves.

INFORMATION THEORY

The method presented here uses all information present in the full data-space (a requirement of information theory [12]) in a probabilistic manner, while keeping cuts and coarse-graining to a minimum. It is defined within the S1-S2 data-space Ω which is parameterised by $x = (S1, S2)$. We seek to determine to what degree a signal can be observed within the data above background. One can identify two relevant functions to be taken as input for the analysis: the first is the actual experimental data, defined as a set of N discrete (S1,S2) points labelled as $x_i^{\mathrm{data}} = (S1_i^{\mathrm{data}}, S2_i^{\mathrm{data}})$, where i runs from 1 to N. The second is the expected distribution of events $\lambda(x)$ which constitutes the theoretical expectation of both the background and possible signal at any point x in the data-space. The experimental data can be thought of as a discrete sample of the theoretical distribution $\lambda(x)$.

We model the data-space Ω by pixelating it into n two-dimensional bins of equal size in S1-S2 given by Δx and labelled with the index j. Within a pixel j at position $x_j = (S1_j, S2_j)$ in the S1-S2 plane there will be a certain number of *experimental* data-points x^{data}. This number will be defined to be n_j. For the same pixel, the *theoretically expected* number of points is given by $\lambda_j = \lambda(x_j)\Delta x$. Hence we can define a Poisson likelihood for all pixels over the whole data-space, by considering λ_j as the mean expectation value of the number

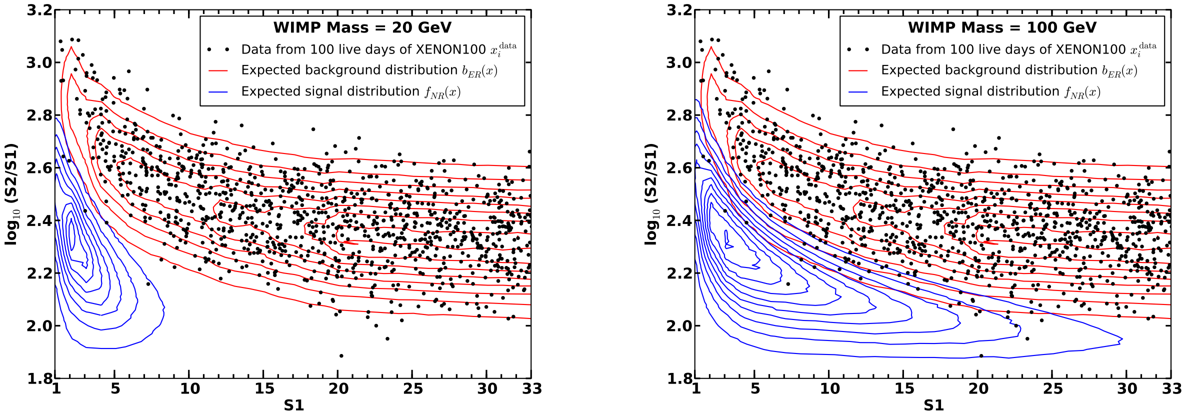

FIG. 1: XENON100 data from 100 live days of running [4] (black dots), the expected distribution of background (red) and WIMP events (blue), with a contour spacing of 10% (12.5%) of the maximum for signal (background). The signals for the two masses are clearly distinct due to their different recoil spectra. Note that $\log_{10}$(S2/S1) has been used in place of S2 for clarity.

of points n_j in each pixel j. Such a Likelihood is given by,

$$\mathcal{P}(d|s)=\prod_{j=1}^{n}\frac{\lambda_j^{n_j}e^{-\lambda_j}}{n_j!}. \tag{1}$$

Here d represents the data and s represents the expected contribution from a possible recoil signal in $\lambda(x)$. We can separate $\lambda(x)$ into its constituent signal $f_{NR}(x)$ and electronic-recoil background $b_{ER}(x)$ parts as $\lambda(x)=f_{NR}(x)\,e^s+b_{ER}(x)$, where s is given in terms of the spin-independent elastic WIMP-nucleon cross-section σ as $s\equiv\ln t\equiv\ln(\sigma/\sigma_0)$ (σ_0 is an arbitrary reference cross-section). Note we assume that ERs are the dominant source of background, and disregard any neutron-induced background, as is done for the analysis used by XENON100 [8]. Dropping this assumption with a well-motivated model could potentially improve the accuracy of our analysis in setting limits.

We must also define a prior for the parameter s. We have no theoretical prejudice on its value and therefore consider a flat prior i.e. assign to all possible log-cross section values s the same a priori probability density function $\mathcal{P}(s)=\text{const}$. Since it extends over an infinite range $\mathcal{P}(s)$ is an improper prior. One can alternatively assume that $\mathcal{P}(s)=1/(s_{\max}-s_{\min})$ for $s\in[s_{\min},s_{\max}]$ and $\mathcal{P}(s)=0$ otherwise. However, provided that $[s_{\min},s_{\max}]$ covers all interesting log-cross-sections, the results do not depend on the precise interval. This has been confirmed for the analysis of XENON100 data using $s_{\min}=-16$ and $s_{\max}=-2$ and directly integrating over the posterior volume. Hence we will use $\mathcal{P}(s)=\text{const}$ throughout this letter.

We can now combine the Likelihood $\mathcal{P}(d|s)$ and prior $\mathcal{P}(s)$ into the joint data and signal probability $\mathcal{P}(d,s)=\mathcal{P}(d|s)\mathcal{P}(s)$. We will work with the information Hamiltonian,

$$H=-\ln\mathcal{P}(d,s)\,\widehat{=}\sum_j\left(\lambda_j-n_j\ln\lambda_j\right), \tag{2}$$

where $\widehat{=}$ means that signal-independent terms have been dropped. The limit can now be taken where $\Delta x\to 0$, so that each pixel can only contain either 1 or 0 data-points. In this limit the Hamiltonian becomes

$$H\,\widehat{=}\int_\Omega \mathrm{d}x\left[f_{NR}e^s-\ln\left(1+\frac{f_{NR}(x)e^s}{b_{ER}(x)}\right)\delta^N(x-x_i^{\text{data}})\right], \tag{3}$$

where the δ-function picks out the positions of the N data-points x_i^{data}. We define $F=\int_\Omega dx\,f_{NR}(x)$, the total number of reference signal (nuclear-recoil) events in the data-space calculated at σ_0.

If the Hamiltonian possesses a classical minimum at s_{cl} then $\partial_s H(d,s_{cl})=0$ and there is a positive identification of signal in the experimental data. In this case the significance of such a discovery is given by the depth of the minimum.

However, if such a classical minimum does not exist, one seeks to define an exclusion limit on the DM-nucleon cross-section (at a certain level of confidence). This can be done by finding the signal parameter $s_{\text{limit}}=\ln(t_{\text{limit}})$ at which the Hamiltonian is increased by a value ΔH from $H(d,s=-\infty)$. We look for the value of t where the likelihood is reduced by an order of magnitude with respect to the case of no DM i.e. $e^{-\Delta H}=0.1$. Such a limit is *numerically* similar to a frequentist limit at 90% confidence, though they are in principle distinct and have different interpretations. By rearranging eq. 3 one obtains an expression for the limiting cross-section,

$$t_{\text{limit}}\equiv\frac{\sigma_{\text{limit}}}{\sigma_0}=\frac{1}{F}\left[\Delta H+\sum_{i=1}^{N}\ln\left(1+w_i t_{\text{limit}}\right)\right], \tag{4}$$

where i sums over all N data-points at positions x_i and w_i are data weights with $w_i=f_{NR}(x_i)/b_{ER}(x_i)$. Eq. 4 contains two terms: the first $\Delta H/F$ is data-independent and gives the absolute limit in the case where no NR events are observed in the data. The second term accounts for potential NR events present in the data, and weakens the limit. We now proceed to discuss how $f_{NR}(x)$ and $b_{ER}(x)$ are determined for the XENON100 experiment in order to obtain a limit.

SIGNAL DISTRIBUTION

WIMP Recoil Spectrum

Potential WIMP events are characterised by their energy dependent recoil spectrum $\frac{dR}{dE}$, parameterised as [13, 14],

$$\frac{\mathrm{d}R}{\mathrm{d}E} = \frac{\sigma(E)}{2m\mu^2}\rho\eta(E,t), \tag{5}$$

where $\sigma(E)$ is the WIMP-nucleus cross-section as a function of energy E, μ is the WIMP-nucleus reduced mass, $\rho = 0.3\,\mathrm{GeV cm}^{-3}$ is the local dark matter density and $\eta(E)$ is the WIMP mean velocity, given by $\eta(E) = \int_{v_{\min}(E)}^{\infty} \frac{f(v+u_e)}{v}\,\mathrm{d}^3v$. The mean velocity is integrated over the distribution of WIMP velocities in the galaxy $f(v)$ boosted into the reference frame of the Earth by u_e. The lower limit of the integration is $v_{\min}(E)$, which is the minimum WIMP velocity required to induce a recoil of energy E. We assume the standard halo model such that $f(v)$ is given by a Maxwell-Boltzmann distribution cut off at an escape velocity of $v_{\mathrm{esc}} = 544\,\mathrm{kms}^{-1}$.

We assume that WIMPs interact identically with protons and neutrons giving $\sigma(E) = \sigma\left(\frac{\mu}{\mu_p}\right)^2 A^2F^2(E)$, where σ is the zero-momentum WIMP-nucleon cross section, A is the atomic mass of xenon, μ_p is the WIMP-proton reduced mass and $F(E)$ is the nuclear form factor (taken to be of the Helm form [13]). Exclusion limits are set on σ for each WIMP mass.

Calculation of S1 and S2 Signals

At a given nuclear-recoil energy E the expected primary ($S1_{\mathrm{exp}}$) and secondary ($S2_{\mathrm{exp}}$) scintillation signals are obtained from the following formulae [10, 15, 16],

$$S1_{\mathrm{exp}} = P\left(E \cdot \mathcal{L}_{\mathrm{eff}}(E) \cdot L_y \cdot \frac{S_n}{S_e}\right) \tag{6}$$

$$S2_{\mathrm{exp}} = 20 \cdot P\left(E \cdot Q_y(E)\right), \tag{7}$$

where $P(x)$ represents a Poisson distribution with expectation value x, $L_y = 2.20 \pm 0.09\,\mathrm{PE keV}^{-1}$, $\frac{S_n}{S_e} = 9.5/5.8$, $\mathcal{L}_{\mathrm{eff}}(E)$ is the relative scintillation efficiency and $Q_y(E)$ is the ionisation yield (we use the best fit functions from [15] here and also perform our own fit of $\mathcal{L}_{\mathrm{eff}}$ to the NR band as in [15]).

To obtain the $S1_{\mathrm{obs}}$ and $S2_{\mathrm{obs}}$ signals observed in the detector, we must include the finite detector resolution and the 20 ns S1 time-coincidence requirement [4, 7]. The latter requires that all events in the XENON100 detector have at least two S1 signals within 20 ns of each other, calculable using the probability distribution of scintillation emission as discussed in the appendix of [15]. Both $S1_{\mathrm{exp}}$ and $S2_{\mathrm{exp}}$ are blurred with a gaussian of width $0.5\sqrt{n}$ for n photoelectrons (PE) to take account of the finite photomultiplier (PMT) resolution. Additionally $S2_{\mathrm{exp}}$ is subject to gaussian fluctuations for the finite size of a single PE, with width 0.58 per PE [15].

Dark matter signal in XENON100

The expected signal distribution for a given WIMP mass in the data-space $f_{NR}(x)$ can now be calculated by Monte Carlo sampling at a value of the reference cross-section $\sigma_0 = 10^{-35}\,\mathrm{cm}^2$ (or $10^{-34}\,\mathrm{cm}^2$ for $m < 10\,\mathrm{GeV}$). The energy range between 1 keV and 60 keV is separated into bins of size $\Delta E = 0.01\,\mathrm{keV}$. For each binned energy E_{rec} we calculate $S1_{\mathrm{obs}}$ and $S2_{\mathrm{obs}}$ a total of N_{rec} times, where $N_{\mathrm{rec}} = \frac{\mathrm{d}R}{\mathrm{d}E}(\sigma_0, E_{\mathrm{rec}})\Delta E$, to obtain the full signal distribution as expected in XENON100.

BACKGROUND DISTRIBUTION

The expected distribution of electronic-recoil background events $b_{ER}(x)$ is determined from fits to ^{60}Co calibration data, as is done in [4, 8]. Although electronic recoil appear mostly Gaussian distributed, the XENON100 collaboration noticed the presence of an anomalous (non-Gaussian) background component [4]. This could be due to double-scatter gamma events, where only one of the gammas contributes to the S2 signal. The distribution is normalised by the total number of expected background events, whose rate takes the constant value of 0.0061 counts per day per kg per keV [17].

RESULTS

Using the expected distributions of signal $f_{NR}(x)$ and background $b_{ER}(x)$ as calculated in the previous sections and shown in fig.1, a limit has been placed on the spin-independent WIMP-nucleon cross section with 100 live days of XENON100 data [4] by solving eq. 4 iteratively for WIMP masses between 6 GeV to 400 GeV. The result is shown as a solid red line in fig. 2 along with its one-sigma $\mathcal{L}_{\mathrm{eff}}$ uncertainty and the limits obtained by the XENON100 collaboration.

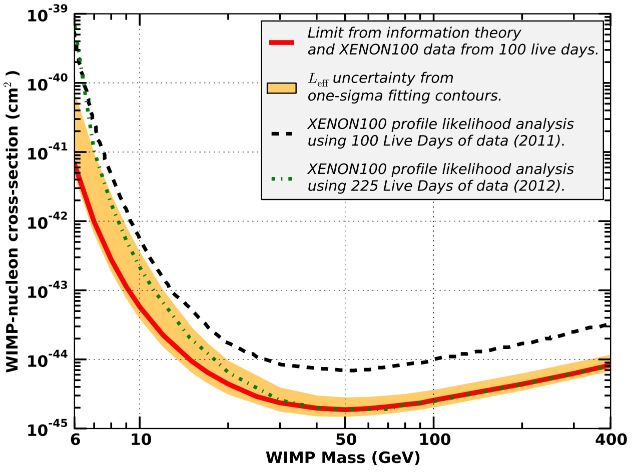

FIG. 2: Limit calculated using the method presented in this letter and 100 live days of XENON100 data [4] (solid red line) with uncertainties due to $\mathcal{L}_{\mathrm{eff}}$ fitting as the shaded region. The 2011 [4] and 2012 [3] exclusion limits obtained by the XENON100 collaboration are shown as a black dashed line and green dot-dashed line respectively.

Clearly the use of this new analytical method has resulted in a sharp improvement in sensitivity over the profile Likelihood method used by XENON100, where we refer specifically to the analysis of XENON100 using bands from here on. In fact we obtain with this Bayesian method and the 2011 data the same exclusion curve as the XENON100 2012 limit [3], for WIMP mass $m > 50\,\mathrm{GeV}$. At low mass the Bayesian method seems to be more powerful. This is due to the fact that the DM signature is very distinct from the electronic-recoil background for low-mass WIMPs, as displayed in fig. 1. Such discrimination at low-mass is not fully exploited by the XENON100 analysis, where the same weights (i.e. the expected ratio of signal $f_{NR}(x)$ to background $b_{ER}(x)$) are defined solely using calibration data for all points within the same band. Hence information on the WIMP recoil spectrum is largely lost in the profile Likelihood method used by the XENON100 collaboration. Additionally this highlights that when identifying points as potential signal or defining a signal region care should be taken to emphasise that this is potentially dependent on the WIMP mass.

For large WIMP masses the extra sensitivity gained can be attributed to the more accurate assignment of weight to the data. The bands used by the XENON100 collaboration [7, 8] ascribe too much weight to points which are actually consistent with the background model, hence resulting in the derivation of an over-conservative limit. Our analysis also appears to benefit from an increased sensitivity relative to other Bayesian works such as [11], where extensive cuts were made. These restricted the data-space to the region where S2 is smaller than the mean of the nuclear-recoil band and resulted in a loss of information and therefore exclusion sensitivity. Regions of data-space where signal could potentially be found are removed in addition to those where the background is expected to be large (shown explicitly in [18]). Such cuts were not made in deriving our exclusion limit, where all data above $S1 = 2\,\mathrm{PE}$ and $S2 = 300\,\mathrm{PE}$ are used.

Our analysis possesses several uncertainties: we use the region of data-space from $S1 = 2\,\mathrm{PE}$ to $S1 = 4\,\mathrm{PE}$, which was cut away in [4]. This has provided us with greater sensitivity to low-mass WIMPs, but may have introduced some extra uncertainties due to the background in this region. Though under a variety of background models the low-mass limit remains robust. We determine L_{eff} (eq. 6) from fits to data, both direct measurements of L_{eff} [19] and fits to ^{241}AmBe calibration data [15]. Hence in addition to a best-fit function one can define contours representing one-sigma deviations consistent with the data [9, 20]. Uncertainties on the exclusion limit due to this one-sigma L_{eff} deviation are shown as the shaded region in fig. 2. They remain of a similar magnitude to those present with the profile Likelihood approach using bands [9], but are not shown by the XENON100 collaboration [3, 4]. A more extensive analysis is performed in [18], including a discussion of the form of L_{eff} used here and its uncertainties from fitting. We note that both the larger uncertainties at low-mass [9] and the extra sensitivity gained in this region are due to the recoil spectra being strongly peaked at lower energies. Hence although the uncertainties are still large at low mass, the extra sensitivity compared to the profile Likelihood method of XENON100 results in a limit which is still stronger, even with a rather extreme one-sigma deviation of L_{eff} from its best-fit.

Astrophysical uncertainties [21–23] have not been discussed here but remain important.

CONCLUSIONS

We have demonstrated that exploiting every pixel in (S1,S2) space instead of using bands has resulted in an exclusion limit which can surpass the 2012 limit obtained by the XENON100 collaboration [3].

The application of the method presented here to the new 2012 data [3] is left to the XENON100 collaboration, with the hope that they can use their expert knowledge of their detector and backgrounds to set an even stronger limit on the spin-independent WIMP-nucleon cross-section.

We hope that the method presented in this letter is intuitive and powerful enough for XENON100 and other experimental collaborations to employ. With a consistent analytical method used by all dark matter direct detection experiments, the current constraints on the WIMP cross-section should be both stronger and clearer.

ACKNOWLEDGMENTS

JHD is supported by the STFC.

[1] CDMS Collaboration, EDELWEISS Collaboration, Z. Ahmed *et al.*, Phys.Rev. **D84**, 011102 (2011), 1105.3377.

[2] D. Y. Akimov *et al.*, Phys.Lett. **B709**, 14 (2012), 1110.4769.

[3] XENON100 Collaboration, E. Aprile *et al.*, (2012), 1207.5988.

[4] XENON100 Collaboration, E. Aprile *et al.*, Phys.Rev.Lett. **107**, 131302 (2011), 1104.2549.

[5] XENON100 Collaboration, E. Aprile *et al.*, Phys.Rev.Lett. **105**, 131302 (2010), 1005.0380.

[6] XENON100 Collaboration, E. Aprile *et al.*, Astropart.Phys. **35**, 573 (2012), 1107.2155.

[7] E. Aprile *et al.*, (2012), 1207.3458.

[8] XENON100 Collaboration, E. Aprile *et al.*, Phys.Rev. **D84**, 052003 (2011), 1103.0303.

[9] J. H. Davis, C. Bœhm, N. Oppermann, T. Ensslin, and T. Lacroix, Phys. Rev. D **86**, 015027 (2012), 1203.6823.

[10] C. Savage, G. Gelmini, P. Gondolo, and K. Freese, Phys.Rev. **D83**, 055002 (2011), 1006.0972.

[11] C. Arina, J. Hamann, and Y. Y. Wong, JCAP **1109**, 022 (2011), 1105.5121.

[12] E. T. Jaynes, *Probability Theory: The Logic of Science* (CUP, 2003).

[13] J. Lewin and P. Smith, Astroparticle Physics **6**, 87 (1996).

[14] D. G. Cerdeno and A. M. Green, (2010), 1002.1912.

[15] P. Sorensen, JCAP **1009**, 033 (2010), 1007.3549.

[16] F. Bezrukov, F. Kahlhoefer, and M. Lindner, Astropart.Phys. **35**, 119 (2011), 1011.3990.

[17] E. Aprile *et al.*, Phys.Rev. **D83**, 082001 (2011), 1101.3866.

[18] J. H. Davis, T. Enßlin, and C. Bœhm, In preparation.

[19] A. Manzur *et al.*, Phys.Rev. **C81**, 025808 (2010), 0909.1063.

[20] A. Manalaysay, (2010), 1007.3746.

[21] C. McCabe, Phys.Rev. **D82**, 023530 (2010), 1005.0579.

[22] A. M. Green, JCAP **1010**, 034 (2010), 1009.0916.

[23] M. Kuhlen *et al.*, JCAP **1002**, 030 (2010), 0912.2358.